Reducing Drag of Body by Adding a Plate

Vladimir A. Frolov[1], Anna S. Kozlova[2]

[1]*Samara National Research University, Department of Aircraft Design and Construction, 443086 Moskovskoye Shosse, Samara, Russia*
[2]*Samara National Research University, Department of Aircraft Design and Construction, 443086 Moskovskoye Shosse, Samara, Russia*

Abstract. This paper focuses on theoretical investigations of the location of a separation point laminar boundary layer on the surface of a circular cylinder. The investigations were carried out by CFD software FlowSimulation. The displacement of the separation point on the surface of the circular cylinder is achieved by installing a flat plate in front of the cylinder parallel to the flow. It was found that the greatest displacement of the separation point to the back of the cylinder is possible when the chord of the plate equals to a quarter of the diameter of the circular cylinder. The flat plate allows not only to change the position of the separation point but also to reduce the drag by about 25%.

1 Introduction

The theme of this article is a topical problem of fluid mechanics, as it solved one of the main questions of aero-hydrodynamics – the drag reducing. The flow around the cross-section of the cylindrical bodies can be wind loads that act on the rocket launcher on the start table, the wind load acting on a tall building with a round shape and also the load, which act on gas and oil pipelines that lie at the bottom of the seas and rivers. Methods that reduce the drag of the body, through the displacement of the point of boundary layer separation include: suction of blowing gas [1, 2], the motion of the wall [3], change the shape of the wall [4, 5], the location of the body near the base body [4, 6]. In this article we investigated the last of these ways – method of displacement of the separation point of the laminar boundary layer on the surface of the circular cylinder by installing a flat plate in front of the cylinder parallel to the flow. The object of investigation was a cylinder with a diameter d=62.5 *mm* that shown in Fig. 1. In front of the cylinder parallel to the stream was installed the flat plate, which had the following characteristics: t=2 *mm* is the thickness of the plate, c is the chord of the plate in *mm*. The plate was located near the cylinder under the meridian angle θ. There is a gap h=d/10 between the cylinder and the plate. Due to the existence of the gap, the effect of the confusor is created [7, 8]. This effect leads to a separation of the flow from the surface of the cylinder and the separation point moves to the back of the cylinder. In Fig. 1, the point of the back of the cylinder is designated ***B***. The thickness t of the plate and the value of the gap h in the study did not change, the relative chord of the plate was set to $\bar{c} = c / d = 0.25$ and $\bar{c} = 0.5$.

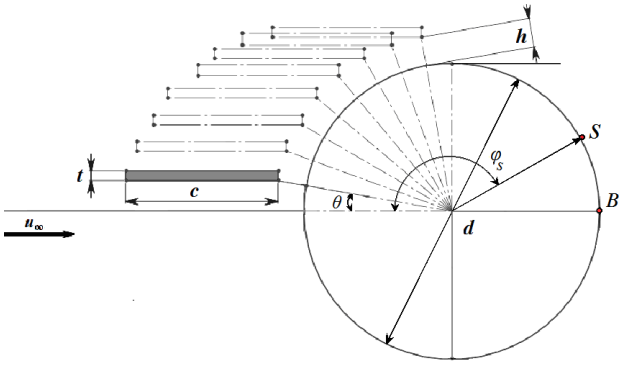

Figure 1. The geometric characteristics of a cylinder with a plate

The position of the separation point S was calculated along the upper surface of the circular cylinder for the combination of the cylinder with the plate, $\varphi_s = x_l / \pi r$ is the polar angle of the separation point, where x_l is the distance along the top of the arc to the point of separation; $r = d / 2$ is the radius of the cylinder.

The calculations were performed for the combination of the cylinder with the plate for the Reynolds number equal to $\mathrm{Re} = \rho u_\infty d / \mu = 10^5$, where $\rho = 1.204$ *kg/m³* is the density of the air; $\mu = 1.81 \times 10^{-5}$ *Pa·s* is the dynamic viscosity of the air at a temperature 293 *K*.

2 Method of the study

The position of separation point were made by CFD in the software FlowSimulation, which is an add-on package to SolidWorks [9]. The integration of the Navier-Stokes equations was obtained in the nonstationary formulation [10]

$$\frac{\partial u}{\partial t}+u\frac{\partial u}{\partial x}+\upsilon\frac{\partial u}{\partial y}=-\frac{1}{\rho}\frac{\partial p}{\partial y}+\nu\left(\frac{\partial^2 u}{\partial x^2}+\frac{\partial^2 u}{\partial y^2}\right),$$
$$\frac{\partial \upsilon}{\partial t}+u\frac{\partial \upsilon}{\partial x}+\upsilon\frac{\partial \upsilon}{\partial y}=-\frac{1}{\rho}\frac{\partial p}{\partial y}+\nu\left(\frac{\partial^2 \upsilon}{\partial x^2}+\frac{\partial^2 \upsilon}{\partial y^2}\right), \quad (1)$$
$$\frac{\partial \rho}{\partial t}+\frac{\partial(\rho u)}{\partial x}+\frac{\partial(\rho \upsilon)}{\partial y}=0,$$

where u is the longitudinal component of the velocity, *m/s*; υ is the transverse component of the velocity, *m/s*; p is the pressure, *Pa*; ρ is the density, kg/m^3; $\nu=\mu/\rho$ is the kinematic viscosity of the air, m^2/s.

The initial condition at the moment time $t=0$ was: $u=u_0(x,y)$, $\upsilon=\upsilon_0(x,y)$, $p=p_0(x,y)$, where u_0, υ_0, p_0 are the functions of coordinates.

The boundary conditions for the system (1) were: 1) the condition of sticking at the surfaces of the solids $u=0$ with $y=0$; 2) change of the tangent and the continuity of the change of the velocity profile $u(y)$; 3) for the plate necessarily condition $\partial^2 u/\partial y^2=0$ at $y=0$; 4) the condition of sufficient remoteness of the boundaries from the zones of disturbance of the flow. Computational domain of the selected models and velocity field are presented in Fig. 2

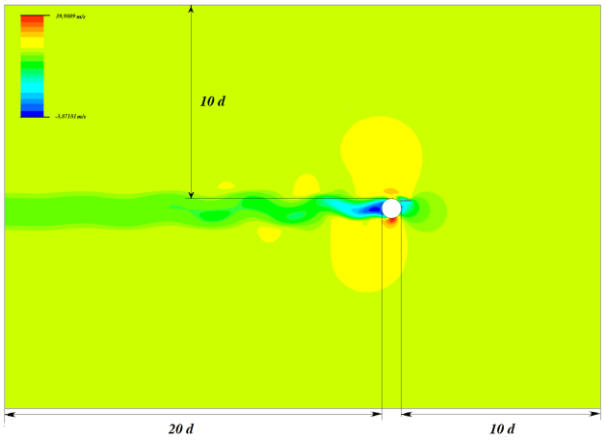

Figure 2. Computational domain of a cylinder with a plate

In the software FlowSimulation equations (1) are simulated turbulent, laminar and transitional flow. For the simulation of turbulent flows is used the definition for small-time: the effect of the turbulence on the flow parameters, large-scale temporal changes are taken into account by introducing appropriate time-derivatives. In the result, the equations (1) have additional members – tension Reynolds, to close the system of equations (1) are the transport equation of turbulent kinetic energy and its dissipation in the framework of the k-ω turbulence model. The transition of laminar flow to turbulent flow is simulated by means of the universal wall functions [9].

The degree of the turbulence for all calculations was taken equal $\varepsilon=0.8\%$, which corresponds to the degree of turbulence of the flow in the wind tunnel of the Samara University.

To solve the problem, the nonstationary model of the physical process is sampled in space and time. To do this, the whole computational domain is covered with grid design and calculated by the method of the finite volumes. The grid block has the shape of parallelepipeds.

The local crushing of the cells shown in Fig. 3.

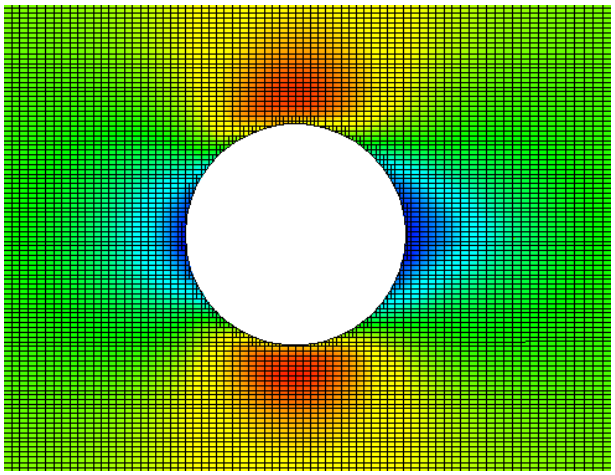

Figure 3. The grid location near the model

In addition to finding the separation point on the upper surface of the circular cylinder was calculated the drag coefficient. The drag coefficient was calculated not for an isolated cylinder only and for the combination of the cylinder with a flat plate. The calculation was carried out based on the method of pulses. According to the theorem of impulse the change of the momentum equals the impulse of the force acting on the streamlined body. The drag coefficient is determined by the formula (2) [7, 8, 10]

$$C_D=\frac{\rho}{q\cdot d}\int_a^b u_1(u_\infty-u_1)dy \quad (2)$$

where q is the impact pressure, u_1 is the velocity at plane $20d$ behind the body, a,b are the boundaries of integration along the y - axis.

3 Results

According to know data [5] for the circular cylinder the dimensionless coordinate of the separation point is equal $S=x_s/(\pi d/2)=0.609$, where x_s is the distance along the arc that forms the surface of the isolated cylinder from the stagnation point to the separation point. The tangential stress is zero $\tau_W=0$ [5, 9] in the boundary layer on the body surface in the separation point.

The simulation gave the value of the relative coordinate of the separation point S=0.619 for the isolated circular cylinder.

Fig. 4, Fig.5 and Fig. 6 shows the velocity, pressure and tangential stress distributions around the circular cylinder, respectively and marked redpoint the separation point.

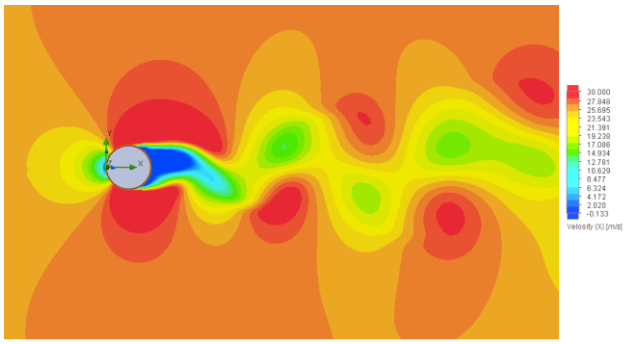

Figure 4. Velocity distribution around a circular cylinder

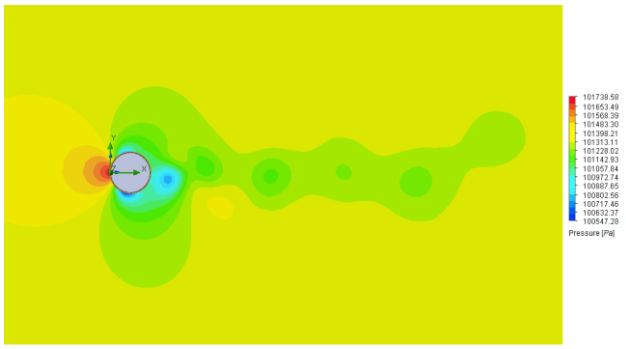

Figure 5. Pressure distribution around a circular cylinder

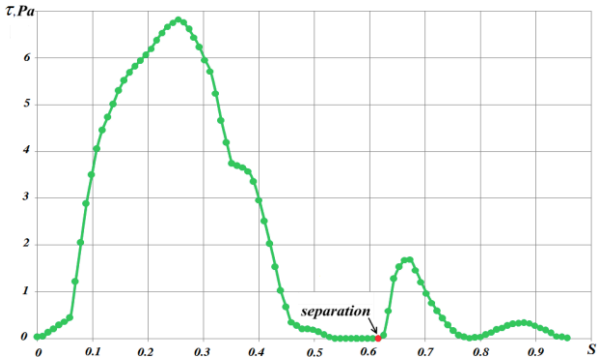

Figure 6. Tangential stress distribution along surface of a cylinder

To verify the results, dimensionless coordinates of the separation points were calculated for elliptical cylinders with different half-axis relationships *a/b*. Table 1 shows the calculated values for the position of the separation point on the elliptical cylinder with different half-axis relationships *a/b*.

Table 1. The calculated values for the position of the separation point

a/b	calculation	experiment [5], [11]
1	0.619	0.609
2	0.708	0.715
3	0.735	0.824
4	0.811	0.845
5	0.865	0.842
6	0.877	-
7	0.860	0.991
8	0.944	0.920
9	0.922	0.920
10	0.982	0.995

Fig. 7 shows the obtained dimensionless coordinates of the separation point in comparison with other authors. Fig. 7 also shows the experimental results of the drag coefficient of elliptic cylinder vs the degree of compression of the ellipse. The experimental data are corresponding to the Reynolds number $Re=10^5$. The experimental results of the drag coefficient C_D were taken from work [11]. Theoretical values of the dimensionless coordinates were taken from Chang's book [5], Schlichting [10] and the experimental results of the values *S* were taken from [12].

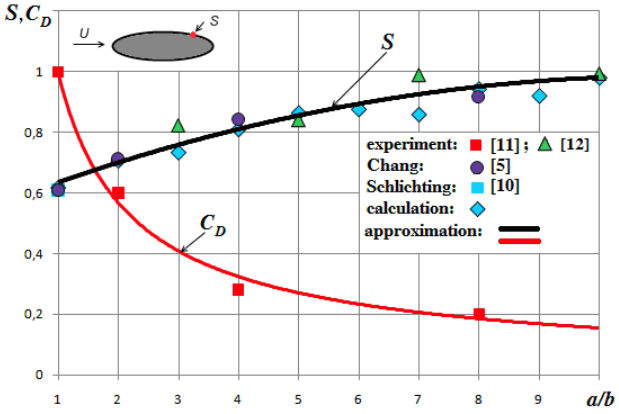

Figure 7. The dimensionless coordinates of the separation point and drag coefficient vs degree of compression on an ellipse

The presented values of the dimensionless coordinates *S* and the drag coefficient C_D clearly demonstrate the dependence of these quantities on the degree of compression of the elliptic cylinder. The presented data in this study indicate that the calculated values for the separation points agree with both the theoretical Chang's results [5] and the experimental results [12]. It is clear from these data that the displacement of the dimensionless coordinates of the separation point *S* to the back of the cylinder leads to a decreasing the drag coefficient C_D. This fact was also noted in works [5, 10].

Further investigation was only performed for a circular cylinder in the presence of the plate. All the calculated values of drag coefficient obtained for the isolated cylinder and combination of the cylinder with a plate. The size of the slit was chosen to be so that the distance from the plate to the surface of the cylinder was always greater than the thickness of the boundary layer.

The calculation of the separation points for combinations of the cylinder with a plate was made for flat plates with relative chords $\bar{c}=0.25$ and $\bar{c}=0.5$. The dimensionless coordinates of the separation points were calculated from the tangential stress distribution of along the upper surface of the circular cylinder and determined by the equality of the tangential stress to zero.

Table 2 and Fig. 8 show the results of calculation of the dimensionless coordinates of the separation point *S* for a circular cylinder in the presence of the plate. Fig. 8 shows the calculating results of the dimensionless coordinates of the separation point *S,* which were obtained for two plates in comparison with data for the isolated cylinder. The specified values of $\theta=0$ *deg* represent a situation in which the symmetry axis of the plate coincides with the longitudinal axis of abscissa.

Table 2. The dimensionless coordinates of separation points for combinations of the cylinder with the plate

θ, *deg*	$\bar{c} = 0.25$	$\bar{c} = 0.5$
0	0.689	0.671
2	0.695	0.699
4	0.715	0.700
6	0.742	0.657
8	0.763	0.627
10	0.766	0.619
12	0.769	0.633
14	0.764	0.659
16	0.750	0.688
18	0.745	0.699
20	0.737	0.715
30	0.723	0.699
40	0.695	0.691
50	0.690	0.685
60	0.670	0.665
70	0.649	0.660
80	0.652	0.650

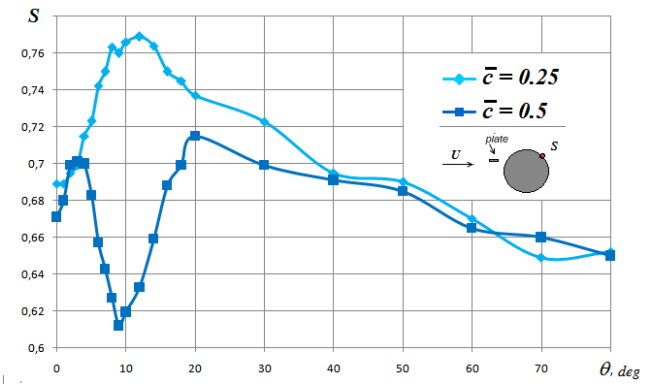

Figure 8. The dimensionless coordinate of separation point for combinations of the cylinder with the plate vs meridional angle

The Table 3 shows the calculated values of the drag coefficient for combination of the cylinder with the flat plate.

Table 3. The drag coefficient for circular cylinder with the flat plate at the different positions of the plate relative to the cylinder

θ, *deg*	C_D	
	$\bar{c} = 0.25$	$\bar{c} = 0.5$
0	0.891	0.863
2	0.890	0.827
4	0.863	0.831
6	0.832	0.893
8	0.791	0.883
10	0.756	0.875
12	0.738	0.846
14	0.744	0.815
16	0.747	0.789
18	0.758	0.754
20	0.767	0.747
30	0.776	0.789
40	0.843	0.838
50	0.957	0.883
60	1.075	0.929
70	1.135	1.001
80	1.177	1.063

Fig.9 and Fig.10 show dependencies dimensionless coordinates of separation point S and drag coefficient C_D vs meridional angle for combinations of the cylinder with the flat plate for dimensionless cords $\bar{c} = 0.25$ and $\bar{c} = 0.5$. The values were obtained as a result of the numerical simulation, some of the values were taken from the works of the authors [7, 8].

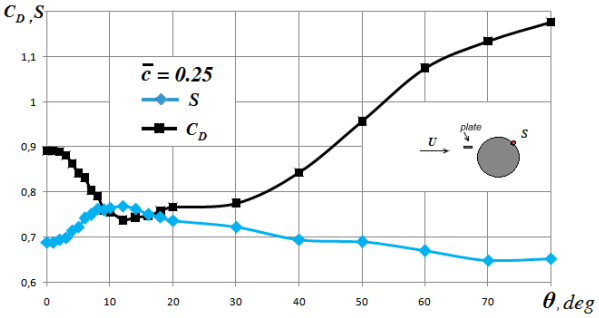

Figure 9. The dimensionless coordinate of separation point for combinations of the cylinder with the plate vs meridional angle

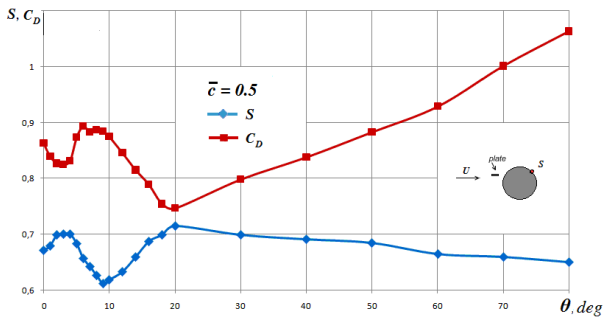

Figure 10. The dimensionless coordinate of separation point for combinations of the cylinder with the plate vs meridional angle

As can be seen from the data in Fig. 7-10 obtained results of the dimensionless coordinates S for the combinations of the cylinder with the plate are greater than for an isolated cylinder. Thus, it can be concluded that the separation point is displacing downward towards the back of the cylinder B on the upper surface of the circular cylinder.

According to the results of the books [5, 10] and the data presented in Fig. 4, the values C_D with increasing coordinates of the separation point S are decreased. It is concluded from the present study that with the increasing value S drag coefficient C_D decreases and with decreasing value S drag coefficient C_D increases.

Thus, the location of the plate in front of the cylinder allows obtaining the displacement of the separation point to the back of the cylinder B and as a consequence the drag reduction.

According to know data [10–12] the drag coefficient of the isolated cylinder is equal to $C_D \approx 1$. Therefore, analyzing the results can say, that for the plate $\bar{c} = 0.5$ in the range meridional angles [70; 80] *deg* and for the plate

$\bar{n} = 0.25$ in the range meridional angles [45; 80] *deg* leads to an increase in coefficient of drag C_D compared to the isolated cylinder. The lowest values of the drag coefficient C_D for the combinations of the cylinder with the plate are noted for the highest values of the dimensionless coordinates *S*.

For the combinations of the cylinder with the plate with dimensionless chord plates $\bar{c} = 0.25$, the separation point gets its highest value *S*=0.769 at the location of the plate at the meridian angle $\theta = 12$ *deg* (Fig. 9). For the combinations of the cylinder with the plate with the dimensionless chord $\bar{c} = 0.5$ the separation point gets its highest value *S*=0.715 at the meridian angle $\theta = 20$ *deg* (Fig. 10). The obtained data are shown in Table 4.

Table 4. The comparison of values of coordinates of separation points for the combination of cylinder with a plate and isolated cylinder

	$\bar{c}$	θ, *deg*	*S*
Schlichting [10]	isolated cylinder		0.610
Chang [5]			0.609
Calculation			0.619
Calculation	0.25	12	0.769
Calculation	0.5	20	0.715

Fig. 11 shows the velocity distribution near the circular cylinder with the plate $\bar{n} = 0.25$, when the meridional angle of the installation of the plate θ=12 *deg*. Fig. 12 shows the pressure distribution around the circular cylinder with the plate $\bar{n} = 0.25$. Fig. 13 shows the tangential stress distribution on the surface of the circular cylinder and marked the red point is the separation point.

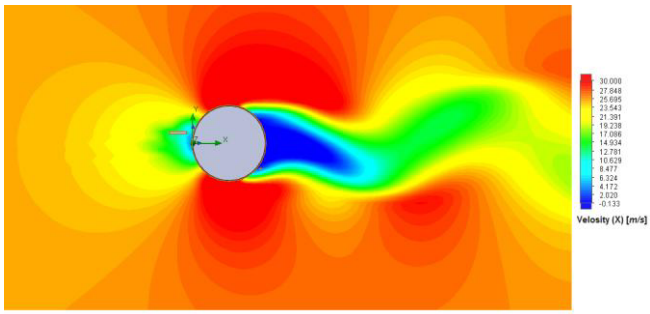

Figure 11. The velocity distribution around the circular cylinder with the plate $\bar{c} = 0.25$

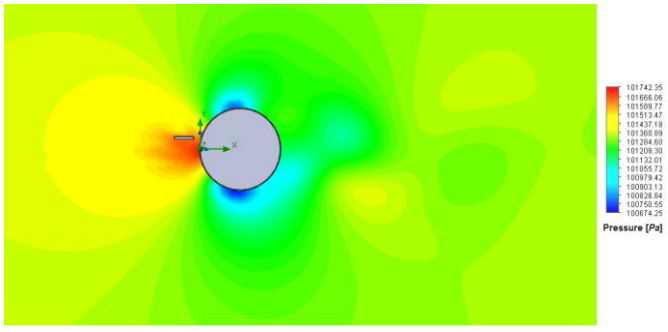

Figure 12. The pressure distribution around the circular cylinder with the plate $\bar{c} = 0.25$

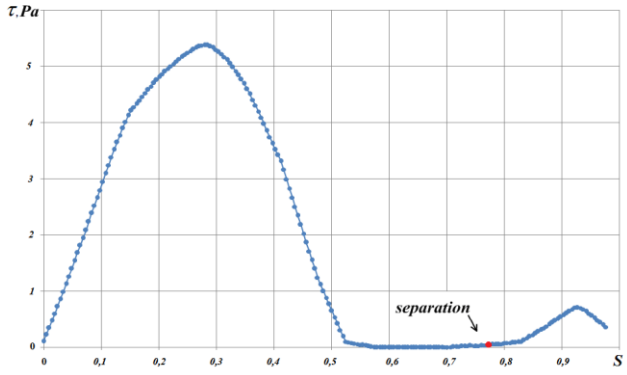

Figure 13. The tangential stress distribution along the surface of the cylinder with the plate $\bar{c} = 0.25$

Fig. 14 shows the velocity distribution near the circular cylinder with the plate $\bar{n} = 0.5$, when the meridional angle of the installation of the plate is θ=12 *deg*. Fig. 15 shows the pressure distribution around the circular cylinder with the plate $\bar{n} = 0.5$. Fig. 16 shows the tangential stress distribution on the surface of the circular cylinder and marked the red point is the separation point.

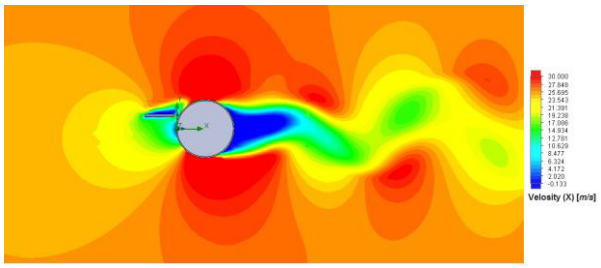

Figure 14. The velocity distribution around the circular cylinder with the plate $\bar{c} = 0.5$

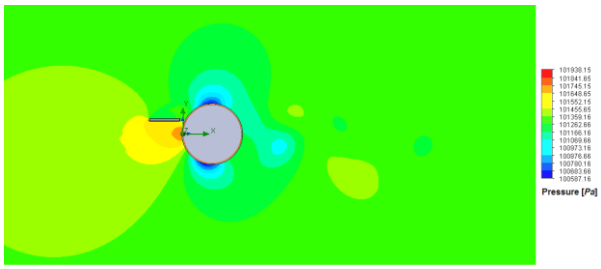

Figure 15. The pressure distribution around the circular cylinder with the plate $\bar{c} = 0.5$

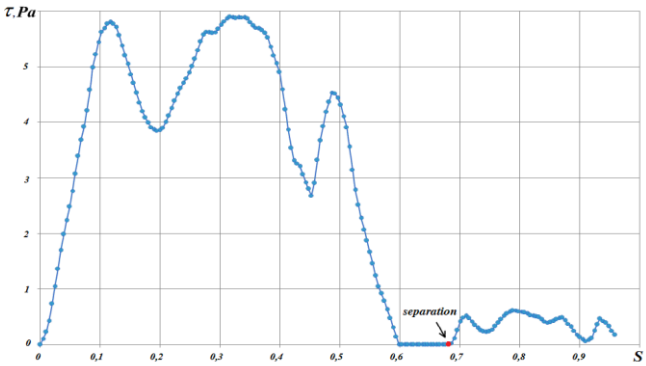

Figure 16. The pressure distribution around the circular cylinder with the plate $\bar{c} = 0.5$

The theoretical values of the angle of disposition of the separation point measured from the stagnation point φ_s are given in works [5, 10, 12]. The results of the calculation angle φ_s and comparison with the known data are given in Table 5.

Table 5. The comparison of the angle for the separation points of the laminar boundary layer on the surface of the combination cylinder with the plate and isolated cylinder

Case Flow	φ_s , *deg*
Isolated cylinder [5, 10, 12]	108.8 –112
Combination cylinder-plate ($\bar{c} = 0.25$)	137.1
Combination cylinder-plate ($\bar{c} = 0.5$)	127.5

According to [10], the theoretical value equals φ_s = 108.8 *deg*. According to the calculation for the combination of the cylinder with the plate $\bar{c} = 0.5$ the separation point is shifted by approximately 18% down on the flow and for the combination of the cylinder with the plate ($\bar{c} = 0.25$) is shifted by approximately 25% down on the flow.

The location of the plate with the chord $\bar{c} = 0.25$ close to the cylinder at the meridian angle θ=12 *deg* is the most optimal and allows achieving a significant displacement of the separation point and as a result of the reducing drag coefficient of the combination of the circular cylinder with the flat plate.

4 Conclusion

The results in the present investigation demonstrate that the displacement of the separation point on the surface of the circular cylinder to the back of the cylinder is made possible due to the location in front of the cylinder the flat plate. The position of the flat plate was studied parallel to the flow and was established at different meridian angles with respect to the longitudinal axis of the cylinder which parallel to the flow. The results show not only the displacement of the separation point of the boundary layer to the back of the cylinder but also reducing drag coefficient of the circular cylinder which can reach 25%.

References

1. V. I. Kornilov, A. V. Boiko,. and I. N. Kavun, Thermophysics and Aeromechanics **22**, No. 4, 413–425, (2015).
2. V. I. Kornilov and A. V. Boiko, Thermophys. and Aeromech. **15**, No.1, pp. 11–27 (2008) (in Russian).
3. T. A. Brungart, G. C. Lauchle, S. Deutsch and E. T. Riggs, Experiments in Fluids **30**, No.4, pp. 418-425 (2001).
4. H.-L. Ma, C.-H. Kuo, European Journal of Mechanics B/Fluids, **59**, pp. 99–114, (2016)
5. P. Chang, *Separation of Flow* (Pergamon, 1970), pp. 69–72.
6. M. Silva-Ortega, G.R.S. Assi, Ocean Engineering, No. 153, pp. 345-352, (2018), doi:10.1016/j.oceaneng.2018.01.116.
7. V. A. Frolov, A. S. Kozlova, *AIP Conference Proceeding* **1893**, 030074 (1-6), (2017), doi:10.1063/1.5007532.
8. V. A. Frolov, A. S. Kozlova, Vestnik of Samara University. Aerospace and Mechanical Engineering **16**, No. 3, pp. 165–172, (2017), doi:10.18287/2541-7533-2017-16-3-165-172.
9. A. A. Alyamovsky, SolidWorks 2007/2008. *Computer simulation in engineering practice*, (BHV-Petersburg, St. Petersburg, 2008), pp. 245–252 (in Russian).
10. H. Schlichting, *Grenzschicht-Teorie* (Publishing Science, Moscow, 1974), pp. 192-194 (in Russian).
11. S. I. Devnin, *Aero hydromechanics of bluff bodies* (Sudostroenie, Leningrad, 1983), pp. 72-90 (in Russian).
12. N. K. Delany, N. E. Sorensen, *NACA TN **3038***, pp. 7–13 (1953).